Biophys. Struct. Mech. 7, 51–63 (1980)

Biophysics of Structure and Mechanism

Cross-Bridge Behavior in Rigor Muscle

E. F. Pate* and C. J. Brokaw

California Institute of Technology, Division of Biology,
Pasadena, CA 91125, USA

Abstract. Properties of the rigor state in muscle can be explained by a simple cross-bridge model, of the type which has been suggested for active muscle, in which detachment of cross-bridges by ATP is excluded. Two attached cross-bridge states, with distinct force vs. distortion relationships, are required, in addition to a detached state, but the attached cross-bridge states in rigor muscle appear to differ significantly from the attached cross-bridge states in active muscle. The stability of the rigor force maintained in muscle under isometric conditions does not require exceptional stability of the attached cross-bridges, if the positions in which attachment of cross-bridges is allowed are limited so that the attachment of cross-bridges in positions which have minimum free energy is excluded. This explanation of the stability of the rigor state may also be applicable to the maintenance of stable rigor waves on flagella.

Key words: Muscle rigor – Cross-bridge model – Insect fibrillar muscle – Cross-bridge stiffness

Introduction

In the absence of $MgATP^{2-}$, muscle is found to be in a "rigor" state characterized by a relatively high stiffness and an inability to perform work. The rigor state has commonly been interpreted as a state in which there are stable cross-bridges between actin and myosin filaments.

When $MgATP^{2-}$ is removed from a muscle, causing it to enter the rigor state under isometric conditions, the muscle can develop a long-lasting rigor tension which may be 50–110% of the normal isometric tension of activated muscle (White 1970; Heinl et al. 1974; Guth and Kuhn 1978; Yamamoto and Herzig

* *Present address:* Department of Pure and Applied Mathematics, Washington State University, Pullman, WA 99164, USA

0340-1057/80/0007/0051/$ 02.60

1978). Detailed measurements of the tension of rigor muscle following length changes have recently been obtained by Kuhn (1978a), using fibrillar flight muscle from the insect *Lethocerus maximus*. The most rapid force transients observed with rigor muscle following small stretches or releases have time constants on the order of a few minutes (at 12° C), several orders of magnitude slower than those of active muscle (Kuhn et al. 1979). A muscle which has developed force in rigor under isometric conditions exhibits an immediate increase in force following a stretch but then recovers to its initial force. After a release force decreases, but the muscle recovers to a force lower than the initial force. In contrast, active muscle typically recovers to its initial steady-state isometric force following either stretches or releases. The transient is simple in vertebrate skeletal muscle but complicated by stretch activation or deactivation in insect flight muscle. A full recovery of force after release is, of course, not possible in an ATP-free, rigor muscle, as it would allow the muscle to continue to perform work in successive releases in the absence of energy input from ATP dephosphorylation. Similar observations have been reported by Marechal (1960) and Mulvany (1975) on iodoacetic acid induced rigor in frog skeletal muscle.

Kuhn interpreted his results to mean that cross-bridge "slippage" – i.e., cross-bridge detachment and subsequent reattachment to a different actin site – to cause force recovery could occur only when the muscle was stretched beyond "yield point" which corresponded to the initial isometric length. The high stability of cross-bridge attachments at or below this yield point was considered to require cooperative interaction between cross-bridges. We describe here a cross-bridge model which does not require cooperative interactions to reproduce the results obtained by Kuhn with fibrillar muscle, and which offers some new insight into the rigor state.

Formulation of a Model for Rigor Muscle

The cross-bridge model developed here derives from the original cross-bridge model of A. F. Huxley (1957), as elaborated more recently by Hill (1974, 1975) and by Eisenberg and Hill (1978). These references should be consulted for general ideas about cross-bridge models which are not explicitly restated here.

A myosin filament is considered to have a row of myosin heads extending from it at intervals d_m. An actin filament runs parallel to the myosin filament, and has sites at intervals d_a, to which myosin heads approaching from a given azimuthal direction can attach to form cross-bridges. When $d_a > d_m$, myosins are in excess, and cross-bridge formation is limited by the number of actin sites. We use $d_a = 38.5$ nm and $d_m = 14.5$ nm (cf. Squire 1977; Holmes et al. 1980). We have also examined models in which actin sites are in excess, and obtained qualitatively similar results. This distinction is important because we begin with the assumption that the rigor state is a state of near-maximal cross-bridge attachment (Huxley and Brown 1967; Miller and Tregear 1972; Haselgrove and Huxley 1973), so that there is no substantial pool of empty actin sites which move

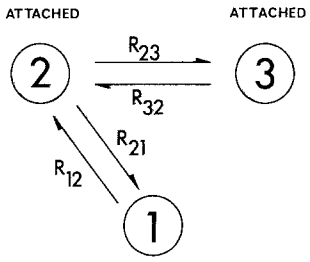

Fig. 1. Cross-bridge states and permitted transitions

into favorable positions for cross-bridge attachment following a release or stretch.

Our model is a three-state model, in which a myosin can be in a detached state (*1*) or in either of two attached states (*2*) and (*3*), with transitions between states permitted as indicated in Fig. 1. This model differs from three-state models for active muscle because in the absence of ATP, state (*3*) does not detach directly to state (*1*).

The distance, parallel to the filaments, between an actin site and a particular myosin can be measured by a variable, x, called the distortion (White and Thorson 1973). The free energy of an attached cross-bridge is a function of x which can be expressed by $A_i(x)$, where i identifies the state. Because of the x-dependence of its free energy, an attached cross-bridge in state i can exert a force, parallel to x:

$$F_i(x) = d\,A_i(x)/dx\,. \tag{1}$$

We have examined models in which the force is a linear function of x:

$$F_i(x) = k_i(x\text{-}a_i)\,, \tag{2}$$

where k_i is the force constant for a particular attached state and a_i is a value of x which gives 0 force. Without loss of generality we can, for convenience, set $a_2 = 0$.

As shown by Hill (1974), the rate functions defined in Fig. 1 are related to the free energy functions by:

$$R_{12}(x) = R_{21}(x)\exp\left([A_1 - A_2(x)]/kT\right)\,, \tag{3}$$

$$R_{23}(x) = R_{32}(x)\exp\left([A_2(x) - A_3(x)]/kT\right)\,, \tag{4}$$

where T is absolute temperature and k (without a subscript) is Boltzmann's constant. Note that the free energy of the unattached state, A_1, is independent of x. The free energy differences can be obtained by specifying two constants, $\Gamma_{12} = A_1 - A_2(a_2)$ and $\Gamma_{23} = A_2(a_2) - A_3(a_3)$, and using Eqs. (1) and (2).

When myosins are in excess, it is convenient to analyze the model by considering the states available to a particular actin site. In order to saturate the

actin sties, the ranges of x for which adjacent myosins can attach to a particular actin site must at least be contiguous, and may overlap, leading to competition between two (or more) myosins for a particular actin site. In order to deal with these competitive interactions between adjacent myosins, it will be necessary to consider at least five possible states of cross-bridge attachment for an actin site – an unattached state and two attached states for each of two adjacent myosins. The specifications used for the model are such that competition between two actin sites for the same myosin can be neglected.

Free Energetic Analysis

Much of the behavior of this cross-bridge model can be obtained by considering the cross-bridge distributions which will be determined by the relative free energies of the states available to a particular actin site.

The subscript j will be used to index the myosins with which a given actin site may interact, with j increasing in the same direction as x. The myosin which initially has distortion in the range $0 < x \leq d_m$ corresponds to $j = 0$. Figure 2a illustrates the free energy levels, as functions of x, for these states. These levels were established by choosing values for Γ_{12}, Γ_{23}, a_3, k_2, and k_3 to give results consistent with Kuhn's measurements.

Since the pattern of free energy levels repeats itself along the length, with period d_m, it is sufficient to illustrate the behavior of cross-bridges that are distributed in an interval of length d_m. A uniform distribution of x-values in this interval is assumed to obtain when a large population of actin sites in a muscle is examined.

At equilibrium we would normally expect that the most probable state for an actin site would be the state with lowest free energy, which is identified by the heavy line in Fig. 2a. To find the complete distribution among the possible states, for a given actin, we let $n_{i,j}(x)$ be the probability of finding a particular actin site bound in state i to cross-bridge j with distortion x. Since $n_{i,j}(x)$ is proportional to $\exp[-A_i(x)/kT]$ and the sum of the probabilities over all possible states at any value of x must be 1 (Hill 1974), we obtain expressions of the form:

$$n_{i,j}(x) = \exp([A_1 - A_i(x)]/kT)\{1 + \sum_{\hat{j}} \exp([A_1 - A_2(x)])/kT) + \sum_{\hat{j}} \exp([A_1 - A_3(x)]/kT\}^{-1}. \quad (5)$$

The values of x in the summations will be $x_0 + \hat{j}d_m$, where x_0 is the distortion to the cross-bridge with $j = 0$. Although the limits on j in the summations are not indicated explicitly, only a few terms in these sums are required; we neglected terms with $n_{i,j}(x)$ values less than 0.025 for all x in the interval under consideration. The equilibrium distribution corresponding to the energy levels in Fig. 2a is shown in Fig. 2b. More than 98% of the actin sites are bound to myosin. Numerical integration of the force resulting from this distribution gives

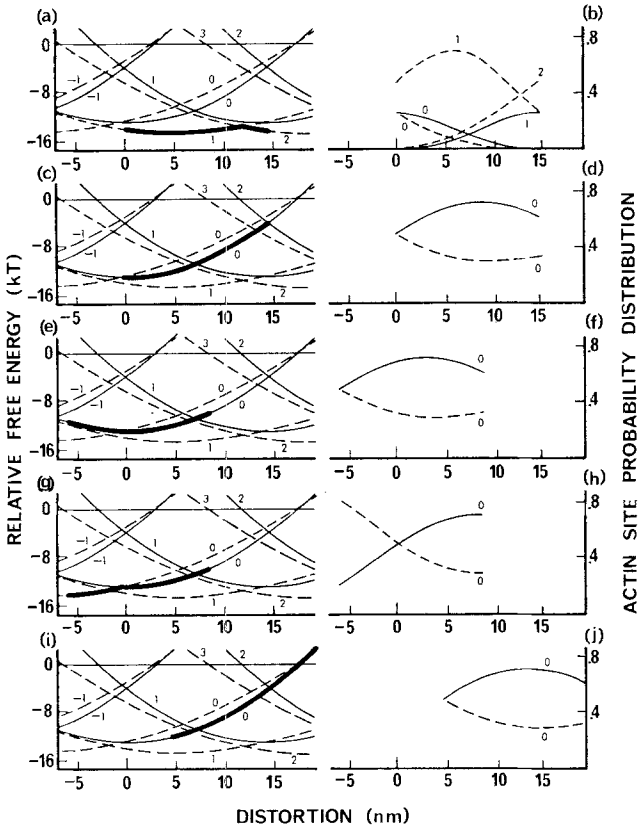

Fig. 2. The left column shows relative free energy levels corresponding to various attachment states for an actin site. The energy level 0 corresponds to the unbound state. Broken lines correspond to state (*3*), solid lines to state (*2*). Numbers beside curves indicate the index for a particular myosin. The most probable states for particular conditions are indicated by heavy lines restricted to a range of width d_m. The abscissa represents distortion for a cross-bridge with $j = 0$. For other myosins, the actual distortion of an attached cross-bridge is obtained by subtracting jd_m. The right column shows actin site probability distributions, $n_{i,j}$, with (*b*) calculated from Eq. (5), and (*d, f, h, j*) calculated from Eq. (5) with $j = 0$ only. The parameters are $d_m = 14.5$ nm, $k_2 = 0.16$ pN/nm^{-1}, $k_3 = 0.08$ pN/nm^{-1}, $a_3 = -9.25$ nm, $\Gamma_{12} = 13.0$ kT, and $\Gamma_{23} = 1.7$ kT

a value which is not significantly different from 0. More generally, the equilibrium distribution for any number of states with force given by Eq. (2) may be shown analytically to produce 0 force. However, when ATP is removed from a muscle to produce a rigor state under isometric conditions, a substantial rigor force is produced, which is maintained for many hours (White 1970; Heinl et al. 1974; Kuhn 1978a). In this situation, the cross-bridge which attaches to a particular actin site is probably not the one which will have the lowest free energy, but is the one which is the most favorably situated for the attachment transition from state (*1*) to state (*2*). As a first approximation, consider that a myosin will attach to form a cross-bridge only if $0 < x \leq d_m$. When a cross-bridge forms in state (*2*), it will make a transition to state (*3*) if this state has a lower free

energy. The most probable state for an actin site will be as illustrated by the heavy line in Fig. 2c, and the actual distribution of states will be as shown in Fig. 2d. Energetically this is not an equilibrium distribution, but under isometric conditions it is indefinitely stable because a transition toward equilibrium would require detachment of a bound cross-bridge and attachment of an adjacent myosin to the actin site. However, for the adjacent myosin, $x \leq 0$, and we have not allowed attachment in this range. Alternatively, the rate of attachment for $x \leq 0$ may be given some small non-zero value, leading to a slow decay of the rigor force. In this case, the stability of the non-equilibrium state producing rigor force is the result of the relative stability of cross-bridges attached to the myosin for which $j = 0$, as well as the low rate specified for attachment to the myosin for which $j = 1$; the rate of approach to the equilibrium state under appropriate conditions will depend approximately on:

$$R_{12}(x_{j+1})R_{21}(x_j)/R_{12}(x_j) .$$

The distribution shown in Fig. 2d will produce an average force of 1.22 pN per actin site. This is equivalent to a force of approximately 166 μN per fiber, consistent with Kuhn (1978a, b) if one assumes the fiber radius is 35 μm, 40% of the fiber is myofibrillar (White 1970), sarcomere length is 2.2 μm, and myosin filaments are 45 nm apart. A release of 6 nm will now cause an immediate change in the cross-bridge distribution to that depicted in Figs. 2e and 2f, and the force will decrease by 0.79 pN. This difference, divided by the length of the release, is a measure of the "immediate stiffness" of the muscle. In this case, it is 0.13 pN/nm^{-1} per actin site. Some cross-bridges in state (*2*) now have x values such that state (*3*) has a lower free energy, so they will undergo a transition to state (*3*), where they will be force-producing. After this process is completed, the cross-bridge distribution will be as shown in Figs. 2g and 2h, and the force per actin site recovers to a value that is 0.64 pN less than the original value before release. This difference, divided by the length of the release, is a measure of the "static stiffness" of the muscle. In this case, it is 0.11 pN/nm^{-1}. The distribution is again stable in time even though it is not at free energy equilibrium. It is closer to the equilibrium distribution shown in Fig. 2a in the sense that more cross-bridges are in state (*3*). They are cross-bridges which correspond to $j = 0$ initially but after a release have distortions which the equilibrium solution determined were appropriate for cross-bridges with $j = 1$. The cross-bridges that remain in state (*2*) are still unable to enter a more stable state (*3*) because they would have to detach, and be replaced by cross-bridges formed by adjacent myosins, but this is still forbidden by the attachment functions.

Figures 2i and 2j show the cross-bridge distribution immediately following a stretch of 4.5 nm from the initial rigor state of Figs. 2c and 2d. To this point, R_{12} has been assumed to be 0 for $x > 14.5$ nm, so that according to Eq. (3), R_{21} must also be 0 in this range, in which case, the cross-bridges stretched to values of $x > 14.5$ nm would be stable. However, if R_{12} for $x > 14.5$ nm is given a non-zero value, but small enough not to alter the previous arguments (such as 1% of the value of R_{12} for $x < 14.5$ nm), cross-bridges stretched to values of $x > 14.5$ nm can now detach to state (*1*) at a slow rate $R_{21}(x)$. Once detached, the rate of

reattachment of the same myosins will be very low, since R_{12} is small for $x > 14.5$ nm. Adjacent myosins ($j = 1$) for which the actin site is in the range $0 \leq x \leq 4.5$ nm will now have much greater attachment rates, and will preferentially attach to the actin site. When this cross-bridge "slippage" process is completed, the cross-bridge distribution will be equivalent to that in Figs. 2c and 2d, but different myosins will be involved. When this distribution is restored, the force wil return to the original value obtained at the "yield point". Therefore the "static stiffness" is 0 for stretches beyond the yield point.

Kinetic Analysis

It remains to demonstrate the existence of a set of rate functions which will give the proper time constants for the initial rise of rigor tension and the tension transients following length changes, consistent with the observations of Kuhn. For this analysis, the differential equations required are of the form:

$$dn_{2,j}(x, t)/dt = -[R_{21}(x) + R_{23}(x)]n_{2,j}(x, t) + R_{32}(x)n_{3,j}(x, t) + R_{12}(x)n_1(x, t)$$

and

$$dn_{3,j}(x, t)/dt = R_{23}(x)n_{2,j}(x, t) - R_{32}(x)n_{3,j}(x, t) ,$$

where

$$n_1(x, t) = 1 - \sum_j n_{2,j}(x, t) - \sum_j n_{3,j}(x,t)$$

and the summations are handled as in the previous section. None of the cases we examined required solution of more than a 5-state system. These equations were integrated numerically by the standard procedure of discretizing the x-coordinate into equal intervals Δx and solving the resulting system of ordinary differential equations for each interval by Gear's routine (Hindmarsh 1974). Results are illustrated in Fig. 3 and 4. All simulations used $\Delta x = 0.5$ nm. Curve O-A in Fig. 3 represents the initial rise of rigor force, obtained by starting with the initial condition that all myosins are detached ($n_1 = 1.0$). $R_{12}(x)$ was specified as $0.11\ s^{-1}$ in the range $0 < n \leq 14.5$ nm, and 0 outside this range. $R_{23}(x)$ is given a lower value of $0.005\ s^{-1}$ and is responsible for the slow rise of force after the first 50 s, as cross-bridges equilibrate between states (*2*) and (*3*).

Experimentally, the initial rise of rigor force is found to be followed by a slower decay to a stable force value (White 1970; Kuhn 1978b). This feature can be incorporated into the model by increasing the range of x values for which attachment can occur, so that the attachment ranges of adjacent myosins overlap. In the overlap region, two adjacent myosins are competing for each actin site. Initially, their attachment will be determined by their relative values of attachment rate, $R_{12}(x)$; which in this case are equal. Subsequently, the

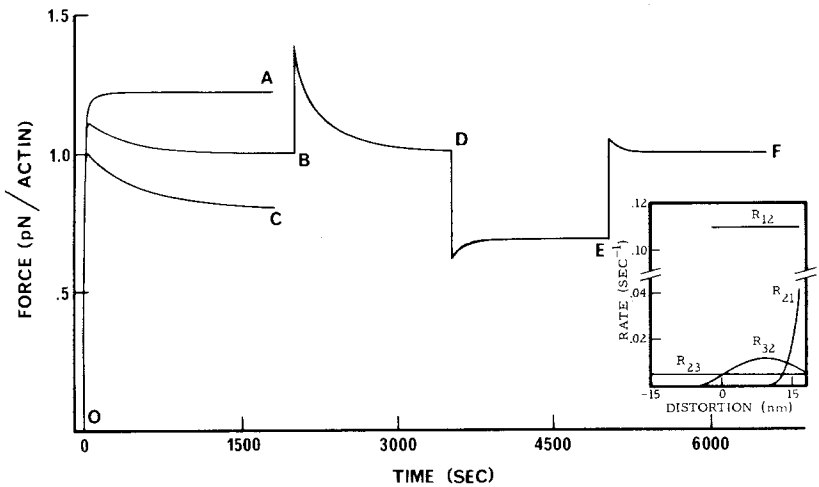

Fig. 3. Force per actin site as a function of time for the rigor cross-bridge model showing the initial rise of force (starting at O), the response to 3 nm stretches (at B and E), and a 3 nm release (at D) for the parameters of Fig. 2. $R_{12}(x)$, $R_{23}(x)$ and the inverse rate functions used for curve O–F are illustrated in the inset

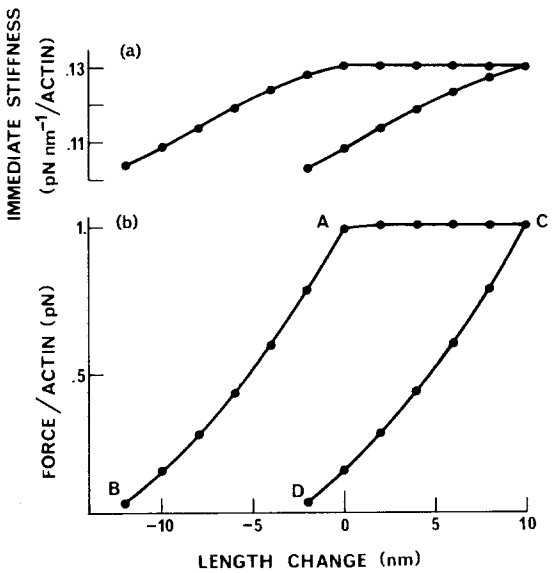

Fig. 4. Response of the rigor cross-bridge model to length changes. Figure 4a shows immediate stiffness at various lengths. Figure 4b shows the force obtained 20 min after each release or stretch

cross-bridges will readjust and the myosins which remain attached will be predominantly the ones with the lower free energy. The result will be that actin with cross-bridges in state $(2,j = 0)$ will make transitions to cross-bridges in states $(2,j = 1)$ and $(3,j = 1)$, at values of x which produce less force (Fig. 2a), so that the average force will decrease.

Curve O-B in Fig. 3 shows results obtained when the range in which $R_{12}(x) = 0.11\ s^{-1}$ was increased symmetrically to $-1.9 \leq x \leq 16.4$ nm, so that there is an overlap region of length 3.8 nm, and curve O-C shows results obtained when the range is increased to $-3.8 \leq x \leq 18.3$ nm. The rigor force decreases to 1.0 pN/actin site when the overlap is increased, as shown by curve O-B. Curve O-B is reasonably similar to experimental results of Kuhn (1978b), so this range has been used for further computations.

With these parameters, few cross-bridges will remain attached to the myosin for which $j = 0$ in the overlap region, since the free energy of the attachment states for the myosin with $j = 1$ is much lower. The value obtained for the steady rigor force will therefore depend strongly on the x value selected for the lower boundary of the attachment range, and will be insensitive to the x value selected for the upper boundary of the attachment range. However, the upper boundary value will determine the magnitude of the peak force which is reached before the force decreases to its steady value.

After establishment of a stable force according to curve O-B in Fig. 3, a 3 nm stretch caused an instantaneous increase in force by 0.39 pN, followed by decay to within 1% of the original rigor force within 20 min. The time course for this decay is largely determined by the values of $R_{21}(x)$ in the region 12.6 nm $\leq x \leq$ 15.6 nm, where the actins which are predominantly in state $(2,j = 0)$ are pulled into the overlap region, and can now reattach to the myosin for which $j = 1$ after detachment. With $R_{12}(x)$ fixed by the time constant for the rise of rigor force, $R_{21}(x)$ must then be determined by the free energy difference between states (*1*) and (*2*), Eq. (3). The result is approximately equivalent to Kuhn's observations following stretch beyond the yield point, but the force decay with our model is nearly exponential, while the force decay observed by Kuhn was nearly linear when plotted against the logarithm of the time after stretch (Kuhn 1978a, Fig. 3). Kuhn suggested that this behavior might be consistent with cooperative binding of myosins.

At D, in Fig. 3, a 3 nm release was imposed, causing an instantaneous decrease in force per actin site by 0.39 pN, followed by recovery within about 3 min to a force value which remained about 0.31 pN below the original rigor force. At E, another 3 nm stretch was imposed, causing an instantaneous force increase, equal to the force decrease at E (to within 5%), followed again by recovery within about 3 min to a force value equal to the initial rigor force. The time constant for recovery following these two length changes is largely determined by the values specified for $R_{23}(x)$, since these length changes below the yield point are followed by redistribution of cross-bridges between states $(2,j = 0)$ and $(3,j = 0)$, rather than by cross-bridge detachment and reattachment.

Further confirmation of the parameters chosen for this model was obtained from the computations summarized in Fig. 4, which match the experimental protocol of Fig. 1 of Kuhn's (1978a) paper which demonstrates a "plastic" response of a fiber to strain. After initial establishment of rigor force as in curve O–B of Fig. 3, a series of 2 nm releases and stretches was imposed on the model, with a 20 min equilibration time allowed after each length change. Figure 4a shows the immediate stiffness measured with each length change, and Fig. 4b shows the force measured at the end of the 20 min equilibration period, just

before the next length change. Both are shown as functions of the change in muscle length. Point A represents the initial values. A series of six releases took the model to point B, and a series of six stretches returned the model along an identical path to point A. Five further stretches took the model to point C, and the initial series of six releases and six stretches was then repeated as shown by line C–D.

An altered experimental protocol allowing for only partial reequilibration of force following a length change was computed. The results (not shown) demonstrated force vs. length behavior different from than in Fig. 4 and an apparent "visoelastic" response, as observed experimentally for frog muscle fibers in iodoacetic acid induced rigor (Mulvany 1975). The series of releases below the yield point and subsequent stretches to the initial length resulted in hysteresis. The magnitude of the force for stretch beyond the yield point increased with decreasing reequilibration period.

The computations summarized in Fig. 4 show that the immediate stiffness decreases as the length is decreased below the yield point, as observed by Kuhn (1978a). Since the immediate stiffness is proportional to the number of cross-bridges in state (*2*) times k_2, plus the number of cross-bridges in state (*3*) times k_3 (Julian and Sollins 1973), this behavior of the model was obtained by having the value of the force constant for the second attached state, k_3, lower than k_2. More of the cross-bridges are in state (*3*) when the muscle is released to a length below its yield point length while the total number of bound cross-bridges remains close to 100%. For stretches beyond the yield point (A–C in Fig. 4) there is no change in immediate stiffness, since the cross-bridge distribution returns to a distribution similar to the initial distribution following a stretch beyond the yield point. The slope of the curves in Fig. 4b is a measure of the static stiffness of the model. The static stiffness also decreases when the length is decreased below the yield point, from 0.098 pN/nm^{-1} for the first release to 0.052 pN/nm^{-1} for the sixth release. As observed by Kuhn, this decrease in static stiffness is considerably larger than the decrease in immediate stiffness, because the magnitude of the force recovery following release increases as the muscle length is reduced. This occurs because near the initial length, many cross-bridges have high x values for which the probability of being in state (*3*) is low both before and after a small release (cf. Fig. 2d). At lengths which give a cross-bridge distribution similar to that shown in Fig. 2h, there will be a greater transfer of cross-bridges from state (*2*) to state (*3*) after release.

Discussion

We have attempted to develop a minimal cross-bridge model which will explain the behavior of rigor muscle without introducing features which are radically different from cross-bridge models suggested for active muscle. We have found one such model which produces force, stiffness, and force transient behavior consistent with the observations of Kuhn (1978a, b).

One feature of this model is the presence of two different attached states for each actin-myosin cross-bridge. These two states have free energy minima at

different distortions, so that a transition between these two states causes a change in the force produced by the cross-bridge. Transitions between these two states can then be responsible for the force readjustments which occur following releases or stretches below the yield point, rather than cross-bridge detachment and reattachment. By assigning different values of cross-bridge force constants, k_i, to these two states, this model also reproduces changes in immediate and static stiffness which occur when the muscle is released to lengths below the yield point, without requiring a change in the number of attached cross-bridges.

The two attached cross-bridge states have force constants in the range suggested by Kuhn et al. (1979) for active *Lethocerus* flight muscle, and are related to each other in a manner similar to the two attached states postulated in models for active muscle. The transitions between these attached states are therefore similar to those suggested to explain the early recovery phase of force transients in active muscle (cf. Huxley and Simmons 1971; Eisenberg and Hill 1979; Eisenberg et al. 1980). However, the rates for these transitions in rigor muscle are several orders of magnitude slower than in active muscle, so the attached states in rigor muscle must be distinct from the attached states which predominate in active muscle. Further information about the differences between these states might be obtained by comparing the behavior of rigor and active muscle during constant-velocity stretches, where the effects of ATP-dependent cross-bridge detachment in active muscle should be minimal.

In this model, the long-term persistence of a non-equilibrium state which generates rigor force is not the result of exceptional stability of the individual force-producing, rigor cross-bridges, relative to the unattached state, and therefore it does not require cooperative, stabilizing interactions between attached rigor cross-bridges. Instead, stability results from the specification of a narrow range of x values for which attachment of a particular myosin to an actin site is possible. For values of x below this range, the attachment rate can be made arbitrarily small, so that the equilibrium state is not accessible by attachment of cross-bridges. The only way in which the equlibrium state can be approached is by allowing cross-bridges to attach in their permitted range of x values, and then releasing the model until the attached cross-bridges have x values corresponding to their state of lowest free energy. This understanding may be the most important result of our work with cross-bridge models for the rigor state.

In our model, the existence of a substantial force in rigor muscle depends on a fairly specific assumption about the range of x values for cross-bridge attachment, which prevents cross-bridges from attaching near their equilibrium value of distortion, where they would produce little force. In fact, to obtain Kuhn's results for force and stiffness, we found it necessary to limit the range of significant attachment rate to $x > -1.9$ nm. It seems unlikely that this feature would occur in muscle either accidentally or as a result of evolution of a capability for producing force in rigor. More likely, it is a reflection of a feature of active muscle, which has evolved to maximize the efficiency of the cross-bridge cycle in a working muscle. It is difficult to determine this feature of cross-bridge attachment from observations on active muscle and therefore very useful to have evidence from data such as Kuhn's on rigor muscle.

Our explanation for the stability of the rigor state may also be applicable to the rigor state in flagella. In flagella, the rigor state obtained in the absence of $MgATP^{2-}$ is indicated less directly than in muscle, by the persistence of "rigor bends" after sudden removal of $MgATP^{2-}$ from actively motile flagella (Gibbons and Gibbons 1974), or by measurements of the bending resistance of flagella (Lindemann et al. 1973; Okuno and Hiramoto 1979; Okuno 1980). In flagella showing persistent rigor bends, the elastic forces which are tending to straighten the flagella must be opposed by forces provided by cross-bridges between the flagellar microtubules. The stable force generated by these cross-bridges presents the same problem encountered in rigor muscle, and may be explained by our cross-bridge model in the same manner.

In this paper, we have simplified our analysis by using a "single actin site" model (Hill 1974) with actin sites for cross-bridge attachment spaced widely at 38.5 nm intervals, along the actin filament. A consequence of this choice is that only about 20% of the myosin heads are attached to actin in the rigor state, consistent with the observations of Offer and Elliot (1978) when the possibility for binding of the two heads to different actin filaments is included. Experimental observations suggesting that 80% or more of the myosin heads are attached in the rigor state (Cooke and Thomas 1980) imply that more actin sites may be available for cross-bridge attachment. The mathematical treatment of multiple actin site models, in which a myosin head can interact with any one of several actin sites (probably with different rate functions) and in which interaction between competing myosin heads on several myosin filaments may be significant, is considerably more complex. We have considered a simple model in order to demonstrate the possibility of a simple explanation of the properties of rigor muscle; however, an analysis of the more complex model with multiple actin sites will probably be required to establish the uniqueness of our explanation.

Acknowledgement. This work has been supported by an NIH grant (GM 21831).

References

Cooke R, Thomas D (1980) Spin label studies of the structure and dynamics of glycerinated muscle fibers: application. Fed Proc 39: 1962

Eisenberg E, Hill TL (1978) A cross-bridge model of muscle contraction. Prog Biophys Mol Biol 33: 55–82

Eisenberg E, Hill TL, Chen Y (1980) Cross-bridge model of muscle contraction; quantitative analysis. Biophys J 29: 195–227

Gibbons BH, Gibbons IR (1974) Properties of flagellar "rigor waves" formed by abrupt removal of adenosine triphosphate from actively swimming sea urchin sperm. J Cell Biol 63: 970–985

Guth K, Kuhn HJ (1978) Stiffness and tension during and after sudden length changes of glycerinated rabbit psoas muscle fibers. Biophys Struct Mech 4: 223–236

Haselgrove J, Huxley HE (1973) X-ray evidence for radial cross-bridge movement and for the sliding filament model in actively contracting muscle. J Mol Biol 77: 549–568

Heinl P, Kuhn HJ, Ruegg JC (1974) Tension responses to quick length changes of glycerinated skeletal muscle fibers from the frog and tortoise. J Physiol (Lond) 237: 243–258

Hill TL (1974) Theoretical formalism for the sliding filament model of contraction of striated muscle. Part I. Prog Biophys Mol Biol 28: 267–340

Hill TL (1975) Theoretical formalism for the sliding filament model of contraction of striated muscle. Part II. Prog Biophys Mol Biol 29: 105–159

Hindmarsh AC (1974) GEAR: Ordinary Differential Equation System Solver, Lawrence Livermore Laboratory Report UCID-30001, Revision 3

Holmes KC, Tregear RT, Barrington Leigh J (1980) Interpretation of the low angle X-ray diffraction from insect flight muscle in rigor. Proc R Soc Lond B207: 13–33

Huxley AF (1957) Muscle structure and theories of contraction. Prog Biophys Biophys Chem 7: 255–318

Huxley AF, Simmons RM (1971) Proposed mechanism of force generation in striated muscle. Nature 233: 533–538

Huxley HE, Brown WJ (1967) The low-angle X-ray diagram of vertebrate striated muscle and its behavior during contraction and rigor. J Mol Biol 30: 383–434

Julian FJ, Sollins MR (1972) Regulation of force and speed of shortening in muscle contraction. Cold Spring Harbor Symp Quant Biol 37: 635–646

Kuhn HJ (1978a) Cross-bridge slippage induced by the ATP analogue AMP-PNP and stretch in glycerol-extracted fibrillar muscle fibers. Biophys Struct Mech 4: 159–168

Kuhn HJ (1978b) Tension transients in fibrillar muscle fibers as affected by stretch-dependent binding of AMP-PNP: a teinochemical effect. Biophys Struct Mech 4: 209–222

Kuhn HJ, Güth K, Drexler B, Berberich W, Ruegg JC (1979) Investigation of the temperature dependence of the cross-bridge parameters for attachment, force generation and detachment as deduced from mechano-chemical studies in glycerinated single fibers from the dorsal longitudinal muscle of *Lethocerus maximus*. Biophys Struct Mech 6: 1–29

Lindemann CB, Rudd WG, Rikmenspoel R (1973) The stiffness of the flagella of impaled bull sperm. Biophys J 13: 437–448

Maréchal G (1960) Rigidité et plasticité du muscle strié en contracture iodoacétique. Arch Int Physiol Biochim 68: 740–760

Miller A, Tregear RT (1972) Structure of insect fibrillar flight muscle in the presence and absence of ATP. J Mol Biol 70: 85–104

Mulvany MJ (1975) Mechanical properties of frog skeletal muscles in iodoacetic acid rigor. J Physiol (Lond) 252: 319–334

Offer G, Elliott A (1978) Can a myosin molecule bind to two different actin filaments? Nature 271: 325–329

Okuno M (1980, in press) Inhibition and relaxation of sea urchin sperm flagella by vanadate. J Cell Biol

Okuno M, Hiramoto Y (1979) Direct measurement of the stiffness of echinoderm sperm flagella. J Exp Biol 79: 235–344

Squire JM (1977) The structure of the insect thick filaments. In: Tregar RT (ed) Insect flight muscle. Elsevier/North Holland, Amsterdam, pp 91–112

White DCS (1970) Rigor contraction in glycerinated insect flight and vertebrate muscle. J Physiol (Lond) 208: 538–605

White DCS, Thorson J (1973) The kinetics of muscle contraction. Prog Biophys Mol Biol 27: 175–255

Yamamoto T, Herzig JW (1978) Series elastic properties of skinned muscle fibers in contraction. Pfluegers Arch 373: 21–24

Received May 28, 1980/Accepted September 2, 1980